

# The surface area and localised 3D roughness of a highly structured surface using X-Ray Computed tomography (XCT)

J.W. McBride<sup>1</sup>, K.J. Cross<sup>2</sup>

<sup>1</sup>Mechanical Engineering, University of Southampton, UK. <sup>2</sup>TaiCaan Technologies Ltd. Southampton, UK.

The characterisation of a highly structured surface is explored. The surface investigated has both high aspect ratio and hidden features. A regular AgNi (80/20) electrical contact has been structured using a scanning electron-beam, with the objective of wear reduction during arcing events. An X-Ray Computed tomography system (XCT) is used to provide data of the whole surface and the data then referenced against a standard calibrated high gauge confocal optical surface metrology system using standard surface metrology software. To allow the surface analysis of the XCT data, the workflow and associated data processing steps are described. The results show that the XCT method provides surface data on the whole surface area including the hidden features, but that the data resolution and associated uncertainty, limits the accuracy of the roughness evaluation. The full surface area is determined using a combination of optical and XCT data.

*Key Words: 3D surface metrology, XCT, surface area*

## Introduction

This paper explores the characterisation of a highly structured surface. We define this as a surface where the height of features is greater than the dimensions of the plane features. Further to this we explore the characterisation of a surface where some of the feature are hidden from the conventional top down measurement methods. Recent investigations have focused on structured surfaces where the height features are much lower than the dimensions of the plane features and where the surfaces are nominal flat, [1,2]. These studies use conventional top down areal metrology limited by the field of view and the angular tolerance of the sensing method. In [3-5] the investigations were on highly structured grooved surfaces (historical mechanical sound recordings) with height features of similar dimension to the width of features. In these studies, large area surfaces (more than 2500 mm<sup>2</sup>) were measured using Con-Focal Scanning (CFS) point sensors and it was shown that the vertical resolution of the sensors used (10 nm) and angular tolerance of the top down scanning were key issues. The high-resolution requirement was linked to the functionality of the surface.

Angular tolerance is linked to the ability of the optical sensing method to return a signal from a sloped non-specular surface. This parameter is critical for a highly structured surface. A surface perpendicular to the light source is defined as a 0° surface, (normally horizontal), while a 90° surface is aligned with the source and referred to as a vertical surface. A 90° (vertical) surface is unable to reflect the incident light from the CFS sensor. Coordinate Measurement Machines (CMM) systems can measure vertical walls using a touch probe, but these systems provide only limited spatial resolution surface data.

In this work we explore the application of a X-Ray Computed tomography system (XCT), to the measurement of a highly structured surface. The calibration of XCT systems for dimensional metrology has many complex aspects and is work in progress in number of research investigations, [6-8]. In this study we investigate the application to surface area and local roughness, by benchmarking the un-calibrated XCT with a reference CFS system.

XCT surfaces are described by point cloud data, as with CMM systems, where each data point corresponds to a unique (x,y,z)

coordinate on a surface, [9]. The data from a CMM are typically a low-density representation of the form of the surface and as such do not allow for surface characterisation; such as wear or surface roughness; the uncertainty of the measurement can be of the same order as the wear, [10]. Auto-Focus and Interferometry methods allow areal measurements over an area limited by the field of view of the optics used. The Con-Focal point Scanning method (CFS) allows for a higher area measurement when compared to the other methods, without the need for data stitching, [9].

## Methods

**The Structured Surface.** The structured electrical contact used is shown in Fig.1. The surface was modified using an electron beam processing method, [11]. A scanned electron beam is used to melt and vaporises the material. Providing that the beam does not penetrate the surface, the vapour pressure of the molten material causes the material to be expelled and a hole formed. The molten material is deposited around the perimeter of the hole. In this study a commercial Ag/Ni (80/20) electrical contact surface is used. The surface investigated has been subjected to arcing with the associated surface transformations of wear, as evidenced in Fig.1 with the darkened region in the centre of the object.



**Fig. 1 Ag/Ni contact processed by electron beam to create a highly structured surface (Diameter 2.5mm).**

**Optical Confocal Scanning (CFS) and X-Ray CT (XCT) Systems.** The optical 3D surface metrology instruments used in this study is the TaiCaan Technologies XYRIS 2020H, [12]. This is a new class of instrument (released in 2020), which combines an ability to measure surfaces with a high angular tolerance, and to scan over large areas, up to (X,Y) 300 x 300 mm with 0.1  $\mu\text{m}$  resolution. The optical sensor used has a 3.3 mm gauge range with a resolution of 0.025  $\mu\text{m}$ , and step height accuracy of 0.012  $\mu\text{m}$ . Data is gathered over a measurement area of 2.6 x 2.6 mm with 1001 data in the X,Y axis, giving a regular grid spacing (pixel resolution) of  $\delta = 2.6 \mu\text{m}$ .

The XCT system used is a Nikon 225 kVp Nikon/Xtek HMX. The data has 8-bit image resolution and a spatial resolution of, 4.8  $\mu\text{m}$  in X, Y and Z, (voxel resolution). The point cloud (STL) data produced requires post-processing to detect and then render the surface. The render settings used with-in VGStudio Max 2.1, are, (1) select a sample of the background and a sample of the volume of interest, (2) use the iso50 surface determination method [6], using an histogram-based image segmentation approach; and (3) select the meshed data options to very precise with no simplification. The XCT process has multiple levels of complexity in terms of error propagation and uncertainty, [6-8].

**Data Processing.** The data format used is a standard 3D point cloud format (STL) for the X-CT system. The XYRIS system generates both STL format data and a standard metrology format (2.5D) data (\*.tai), where a single value height (z) is associated with a single X,Y position in the measurement plane. Both formats are imported into BEX, the surface analysis software package [13], for analysis of the dimensional, surface roughness and surface area data. For the XCT data there is an initial 2 stage process is to remove the manifold, which contains both the upper surface and the lower surface of the sample, as a closed manifold; so that only the upper surface remains. The surface is levelled and for the 2D section the (STL data) surface intersections determined relative to the selected 2D line section. A 2D gaussian filter can then be applied for determination of 2D roughness parameters. The measured surface is shown in Fig. 2.

For 3D surface roughness, the STL data surface is re-sampled onto a user defined fixed grid (\*.tai) data format. This action removes all hidden surfaces, as the algorithm selects the highest value with multiple z values. A section of the peak surface identified in Fig. 2, as peaks 1-4 are then segmented using a user selected radius (0.1mm). A 0.08 mm gaussian filter applied, allowing the generation of 3D roughness parameter ( $S_a$ ).

**Characterisation.** 3D roughness parameters are basic descriptors proving limited information on the nature of a surface. In this application both spatial and amplitude information, along with some function describing the functionality of the surface is required. In this study there are two primary parameters, the local  $S_a$  roughness of a peak as described above and the surface area. The surface area can be defined using the texture ratio,  $S_{dr}$  parameter, which describes the percentage texture increases from a perfectly smooth surface. For a smooth, perfectly flat surface, the value is 0. For highly structured surfaces the percentage value can more than 100%, we have therefore used the absolute ratio of the measured surface area, over the project area, and call this  $S_{ap}$ . For an ideal smooth plane surface, the texture ratio ( $S_{ap}$ ) is 1. © TaiCaan Technologies Ltd.

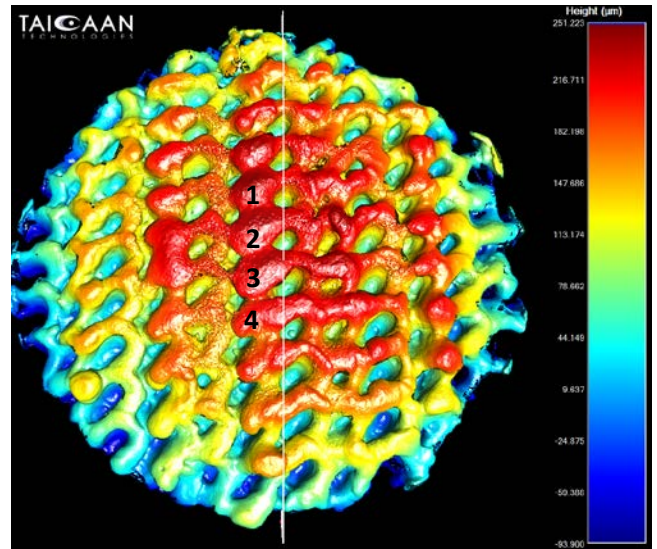


**Fig. 2, XCT data using Jet colour scale (max 251 to min -93.9  $\mu\text{m}$ ). The location of Peaks 1-4. The white line in the upper image offset to show hole features, corresponding to the cross-section data in Fig. 4.**

For highly structured surfaces the  $S_{ap}$  value can be significantly higher than 2. Where,  $A_s$  is the surface area and  $P$  the projected area.

$$S_{ap} = \frac{A_s}{P}$$

In summary, the following parameters are compared in both XCT and CFS data:

1.  $S_{ap}$ , as defined, over a fixed 1mm radius projected area, taken from the highest point closest to the centre of peak 3 in Fig.2.
2.  $S_a$ , the amplitude of the roughness of the surface, over a selected peak region (1-4) using a 0.08 mm Gaussian filter length.
3. To investigate the dimensional characterisation, the peak to valley dimension of the 4 closest holes to each of the 4 peaks labelled in Fig.1 are compared.

## Results and Discussion

**XCT data.** The XCT data is shown in Fig 2 when loaded and process as STL data in BEX<sup>®</sup>. The image uses a height colour scale to show the complexity of the surface. The colour scale allows hole features to be identified as approximately 0.2 mm deep with the hole features at the same approximate spacing. In addition, it is evident that there are regions of overhanging material around the holes.

**CFS data.** The higher data resolution of the CFS scanning data is evident in Fig. 3. The top down view is aligned to show the same features as Fig. 2, with contours used to enhance the image. A data inclusion area of 1mm radius has been applied centred on peak 3, used for the evaluation of the surface area parameter ( $S_{ap}$ ). The cross-sections corresponding to the white lines in Fig's. 2 and 3 are shown in Fig. 4; and the results shown in Table 1.

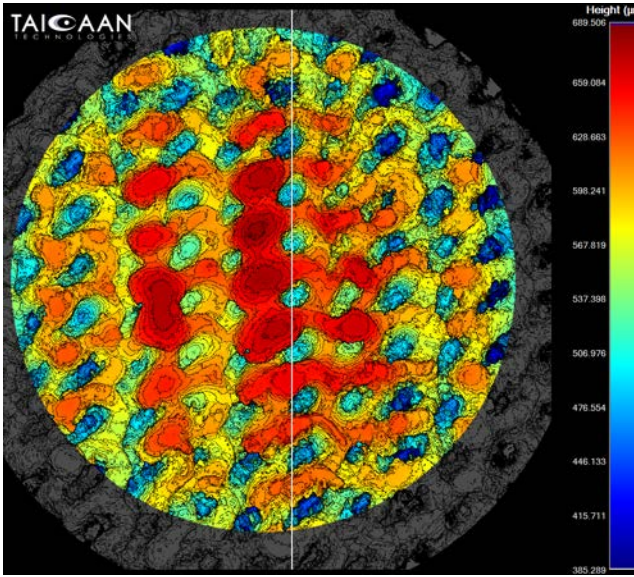


**Fig.3 CFS data, max 689.5 to min 358.3 μm. Data length 2.6mm with a spacing  $\delta = 2.6 \mu\text{m}$ . The vertical cross section (white line) is offset to match the section in Fig .2, see Fig 4.**

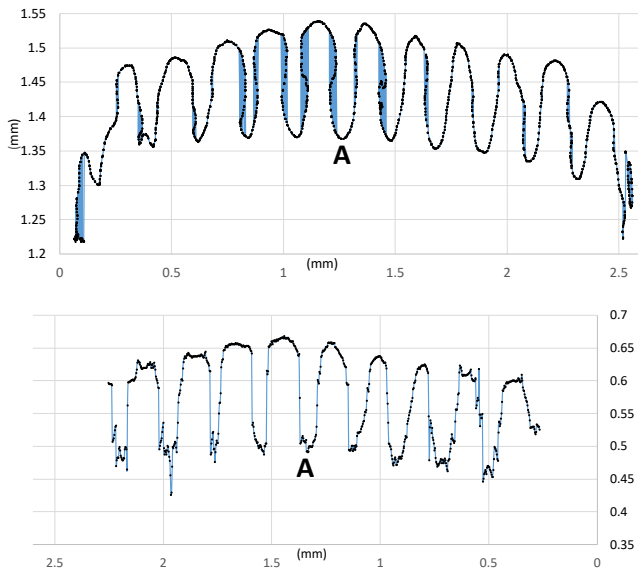


**Fig.4, all axis (mm), XCT (a) upper, cross section data with overhang data; CFS (b) lower, (note the CFS data is rotated by 180 degree in Fig. 3, to match the XCT axis).**

**Cross Sections.** The cross sections for both the XCT and CFS data are shown in Fig 4 (a) and (b) respectively. The data is used to detail the hole features to the right of the peaks numbered in Fig.1. The upper XCT figure shows regions of overhanging data with the blue shading. The lower CFS data is unable to show the overhang, but has a higher spatial resolution as evidenced by the greater details of the surface. For comparisons the hole at position A is identified on both cross sections. Further details of the significance of the overhang and hidden surface is shown in Fig.5 with a cross section through peak 3.

**Surface Area.** To define the surface area, it is first necessary to constrain the projected area. The latter being the area over which the surface area is determined. BEX<sup>®</sup> allows the user to define a selected area based on a user defined 1mm radius from the highest point in peak 3 is shown in Fig. 3. The method is repeated 10 times and the resultant average shown in Table 1.

The surface area data for the XCT is shown in Table 1, as two values, the first (2.5) is for the STL data re-samples onto a fixed grid with a single Z height value for each point, the second (3D) is calculated directly from the STL data format and includes the area of the hidden surface. To constrain one of the variables and normalise the data for comparison the XCT data is re-sampled in BEX<sup>®</sup> to the 2.5D (\*.tai) format, to match the CFS data size of 1001 x 1001. In addition, the algorithm used (BEX) only uses the higher surface value thus removing the overhanging data to match the CFS data in Fig.4. The XCT surface area parameter ( $S_{ap}$ ) is lower than that for the CFS data, in Table 1. A combination of both increased surface amplitude roughness and data sampling ( $\delta$ ), are known to increase surface area. The higher CFS surface area is therefore a function of the increase surface roughness.

To account for the hidden surface area, the following method is proposed. We define 3 surface area parameters, linked to the method used (using the same projected area of a 1mm radius);

$S_{ap}$  (1) is from CLS data, with no hidden surface, and higher surface detail, (3.01 in Table 1).

$S_{ap}$  (2) is from XCT 3D data including the hidden surface, (1.9 in Table 1).

$S_{ap}$  (3) is from the XCT 2.5D data, re-sampled from  $S_{ap}$  (2) to the same grid spacing as  $S_{ap}$  (1), (1.86 in Table 1).

Note;  $S_{ap}(2) > S_{ap}(3)$ , as it includes the area of the hidden surface; and  $S_{ap}(2) - S_{ap}(3)$  is the hidden surface area.

To accommodate the hidden surface area, and the surface area of the rougher surface (CLS), we define a resultant  $S_{ap}'$ ;

$$S'_{ap} = S_{ap}(1) + S_{ap}(2) - S_{ap}(3)$$

$$A_s = S'_{ap} P$$

**Dimension Analysis.** With no reference marks or registration points on the surface, to enable dimensional comparison, the

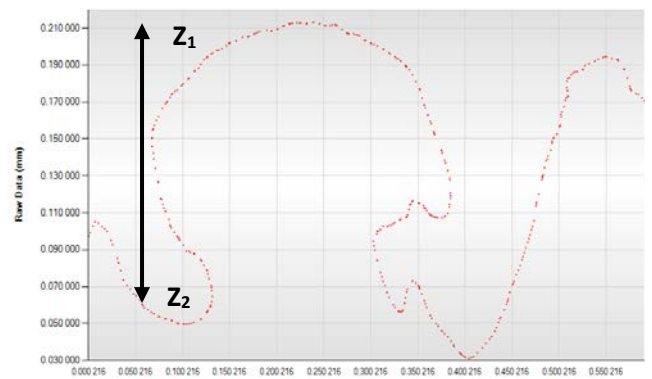


**Fig. 5 XCT detail of a peak 3 with under-cut surface and the vertical visible position of the hole ( $Z_1$ - $Z_2$ ) indicated by the black line used to compare with CFS.**

**Table 1. Results**

Parameter	Sap	PV mean	Sq(1)	Sq(2)	Sq(3)	Sq(4)
CFS	3.01	0.1757	4.97	3.37	2.07	2.10
XCT (2.5D)	1.86		3.42	2.52	1.77	1.42
XCT (3D)	1.9	0.1781				

following method is adopted. For each peak (1-4) in Fig 2, the average depth is measured as the distance between the peak and the hole bottom, from the 4 holes diagonally from the peak. The Peak to Valley (PV) value present in Table 1 is the average over all 4 peaks. This method limits the dimensional analysis to the Z data only. For the XCT 3D data the process is modified as shown in Fig. 5, as the lowest point is hidden from the top down view. The height used is limited to that visible from above, as ( $Z_1-Z_2$ ). The results show that the XCT hole depth is consistently higher than the CFS data, with a range between 4.35 and 0.1  $\mu\text{m}$  over the 4 peaks, with an average of +3.36  $\mu\text{m}$ . Table 1 shows the Peak to Valley value (PV), as the average of the 4 holes around the 4 peaks, it shows the higher XCT (+3.36) value. It is noted that the XCT system is uncalibrated, while the CFS value is traceable to a standard step height UKAS artefact.

**Surface Roughness.** To determine the roughness a region of 0.1 mm radius is used on each of the 4 peaks identified in Fig.2. For the XCT data the converted (\*.tai) format is used as described in the surface area measurement. A 3D 80  $\mu\text{m}$  gaussian filter is then applied and the Sa (surface amplitude roughness) determined and shown in Table 1. As noted above on all 4 peaks the roughness is greater in the CFS data. This is because the XCT data voxel resolution leads to a smoothing of the natural surface, as apparent in the Fig.4 cross sections. The higher roughness of each of the selected peaks also supports the higher surface area measurement of the CFS data.

## Conclusions

The paper describes a methodology for post processing of XCT generated surface data for surface characterisation. Surface area is determined from STL point cloud data while roughness parameters require the application of a 3D Gaussian filter on a regular fixed grid with a single Z height value.

The highly structured surface investigated shows an advantage of the XCT data, in rendering the overhanging features. The higher spatial resolution of the optical CFS data means that the surface area calculation is influenced by the higher surface roughness, while the hidden surfaces will act to increase the surface area in the XCT data. To determine the real surface area, it is proposed that the CFS optical surface area is supplemented with the XCT hidden surface area.

## References

1. N. Senin, L.A. Blunt, R. K Leach, S Pini, "Morphologic segmentation algorithms for extracting individual surface features from areal surface topography maps". Surf. Top. Metrol. Prop. 1, 2013, 015005 pp. 1-11.
2. G. MacAulay, Ph.D Thesis, "Characterisation of structured surfaces and assessment of associated measurement uncertainty", 2015.
3. P.J. Boltryk, M. Hill, J.W. McBride, A. Nasce, "A comparison of precision optical displacement sensors for the 3D measurement of complex surface profiles", Sensors and Actuators A: Physical, 142, (1), 2008, pp. 2-11.
4. P.J. Boltryk, Hill M, McBride, J.W. "Comparing laser and polychromatic confocal optical displacement sensors for the 3D measurement of cylindrical artefacts containing microscopic grooved structures", Wear, 266, (5-6), 2009, pp. 498-501.
5. [www.taicaan.com/sound-archive-project](http://www.taicaan.com/sound-archive-project)
6. J.J. Lifton, A. A. Malcolm, J. W. McBride, "On the uncertainty of surface determination in X-ray computed tomography for dimensional metrology", Measurement Science and Technology, 2015, 26 (3), 03500.
7. J.J. Lifton, A.A. Malcolm, J.W. McBride, "A simulation-based study on the influence of beam hardening in X-ray computed tomography for dimensional metrology", Journal of X-ray Science and Technology 23 (1), 2014, pp. 65-82.
8. W. Sun, S. Brown, N. Flay, M. McCarthy, J.W. McBride, "A reference sample for investigating the stability of the imaging system of x-ray computed tomography", Measurement Science and Technology 27 (8), 085004
9. J.W. McBride "Confocal-Scanning of Surfaces", 2020, [www.taicaan.com/publications](http://www.taicaan.com/publications)
10. P.J. Bills, R. Racasan, R.J. Underwood, P. Caan, J. Skinner, A.J. Hart, X. Jiang, L. Blunt, "Volumetric wear assessment of retrieved metal-on-metal hip prostheses and the impact of measurement uncertainty", Wear, 2012, pp. 274-275.
11. B. A. Dance, B.G Buxton, "An introduction to surf-sculpt technology, new opportunities, new challenges", Proceedings of the 7th International Conference on Beam Technology, 2007, pp. 75-84
12. [www.taicaan.com](http://www.taicaan.com) Products; XYRIS 2020H
13. BEX ® <https://www.taicaan.com/software>